Published in final edited form as:
Expert Opin Med Diagn. 2009 November 1; 3(6): 673–687. doi:10.1517/17530050903140514.

Advances in Cardiovascular MRI for Diagnostics: Applications in Coronary Artery Disease and Cardiomyopathies

Michael Salerno, MD, PhD and **Christopher M Kramer, MD**

Abstract

Background—Cardiac magnetic resonance (CMR) imaging has emerged as an important cardiac imaging technique for the evaluation of multiple cardiac pathologies.

Objective/Method—The goal of this review is to describe recent advances in techniques which have extended the potential applications of CMR. The focus will be on the clinical applications of CMR for the evaluation of coronary artery disease and heart failure/cardiomyopathies which are major causes of morbidity and mortality worldwide.

Conclusion—CMR provides unique tissue characterization which is not available from other imaging modalities and has demonstrated important diagnostic and prognostic information in many forms of heart disease.

Keywords

Cardiac Magnetic Resonance Imaging; Cardiomyopathies; Coronary Artery Disease; Diagnostic Imaging

1. Introduction

Cardiovascular magnetic resonance (CMR) has become a clinically important tool for the evaluation of known or suspected heart disease. Advances in both scanner hardware and novel pulse sequences continue to improve the diagnostic utility of CMR. The advantages of CMR include the lack of non-ionizing radiation, the large variety of tissue contrast mechanisms, and the ability to image the heart in any arbitrary direction. A comprehensive CMR study is a combination of techniques that enables physicians to evaluate cardiac structure, function, tissue characteristics, perfusion, and scarring or fibrosis. The components of the examination are tailored to the particular diagnostic question at hand. This article will review advances in the diagnostic abilities of CMR for evaluating heart disease. We will specifically review advances for the clinical evaluation of coronary artery disease (CAD) and congestive heart failure/cardiomyopathies, the most common causes of morbidity and mortality in the U.S.

2. Overview of CMR techniques and Recent Advances

The versatility of CMR is due to the fact that the imaging characteristics can be changed by choosing a specific pulse sequence and parameters which alter the precise timing of radiofrequency (rf) pulses and magnetic field gradients within the scanner. One of the

Corresponding Author: Christopher M, Kramer, Professor of Radiology and Medicine, Director, Cardiovascular Imaging Center, University of Virginia Health System, P.O. Box 800170, Charlottesville, VA 22908-0170, USA.

Declaration of interest

CM Kramer is a consultant for Siemens Medical Solutions and received a research grant from Astellas. M Salerno states no conflict of interest and have received no payment in preparation of this manuscript.

challenges of CMR is that the heart position changes due to intrinsic cardiac motion and bulk motion from respiration. These effects are typically minimized by timing image acquisition to the cardiac cycle by ECG gating and minimizing respiratory motion with breath holding. There are multiple ECG-gated acquisition modes: Single-shot techniques create a single image each heartbeat, segmented techniques acquire data for a single image over multiple heart-beats, and cine techniques create movies of cardiac motion with data acquired at multiple cardiac phases over multiple heart-beats.

2.1 Anatomic Imaging

A typical imaging protocol will begin with single-shot "scout" images acquired to provide initial localization of cardiac structures. Anatomic images of the chest covering the heart and great vessels are then obtained by a series of single-shot sequences using so called "dark-blood" or "bright-blood" techniques. Dark-blood imaging is usually performed with a single-shot turbo spin echo (TSE) based pulse sequence,[1, 2] while bright blood imaging is performed with single-shot Steady State Free Precession (SSFP) pulse sequence. These sequences have largely replaced older segmented TSE techniques.

2.2 Functional Imaging

Functional images of the heart contraction throughout the cardiac cycle are then obtained in multiple orientations using cine-SSFP pulse sequences. SSFP has become the reference standard because of its superior contrast between myocardium and the blood pool.[3] Conventional cine-gradient echo (GRE) pulse sequences have poorer contrast between the blood pool and myocardium, but remain useful for evaluating valvular disease due to their inherent dephasing of the regurgitant blood signal. Quantitative evaluation of cine-images provides accurate and reproducible measures of ejection fraction (EF), and cardiac chamber dimensions.[4, 5] The application of parallel imaging techniques which reduce the amount of data that needs to be collected, has improved the temporal and spatial resolution of single-breath hold cine-SSFP imaging.6 Techniques for real-time cine imaging, which enable imaging of myocardial function without ECG-gating or breath-holds, have extended the utility of CMR to patients with cardiac arrhythmias or who are unable to hold their breath.7 Currently 3-D parallel techniques are being developed which can perform cine images of the whole heart in a single breathhold.[8] Quantification of regional myocardial function can be performed using techniques such as myocardial tagging[9], DENSE[10, 11], and HARP[12] which can provide information about regional displacement and strain.

2.3 Tissue Characterization

Additional sequences in which image contrast is weighted by intrinsic magnetic relaxation times such as T_1, T_2, or T_2* relaxation times may be obtained depending on the specific application. T_1 weighted images are generally obtained using "dark-blood" breath-held segmented TSE pulse sequences. In most studies T2-weighted imaging has been performed using a "dark-blood" T2-weighted TSE pulse sequences.13 These types of pulse sequences suffer from multiple artifacts which can be mistaken for pathology. This has somewhat limited their clinical robustness. Over the last few years there has been improvement in the pulse sequences for T2-weighted imaging of the heart. Kellman et al. demonstrated high quality bright-blood T2-weighted SSFP images using a T2-weighted preparation.[14] This pulse sequence eliminates many of the artifacts mentioned above, but has reduced signal-to-noise ratio (SNR) compared to TSE pulse sequences. A further improvement is the $ACUT_2E$ pulse sequence described by Aletras et al. which combines the advantages of both TSE and SSFP pulse sequences and creates T2 weighted images with excellent image quality and SNR similar to traditional TSE pulse sequences.[15]

Iron overload of the myocardium can be assessed by mapping the T2 or T2* relaxation times which are reduced in the presence of iron. Images sensitive to T2* may be obtained with a segmented GRE pulse sequence where images of the heart are collected with multiple echo times (TE) over a single-breath hold.[16] From these images, the T2* of the myocardium can be determined. T2* weighted techniques can suffer from motion artifacts, and T2* is affected by other parameters besides myocardial iron. For these reasons, a new TSE-based pulse sequence has been developed to create maps of the myocardial T2 which may be more robust to motion than the older T2* pulse sequences.17

2.4 Perfusion

Images of myocardial perfusion can be obtained with high spatial and temporal resolution during first pass of gadolinium contrast agents. These contrast agents shorten the T1 relaxation time of blood. On heavily T1 weighted pulse sequences regions of the heart which are well perfused appear bright, whereas regions of reduced perfusion appear dark. Current perfusion protocols use non-selective saturation recovery-prepared pulse sequences followed by rapid single-shot imaging.[18–21] There are various data-acquisition strategies which have differences in their temporal resolution and robustness to various artifacts. To further improve temporal resolution parallel imaging techniques are generally used.[22] Multiple studies have compared various pulse sequences, but there has been no clear consensus on the optimal technique.[23, 24]

While the majority of published studies have been at 1.5T, multiple investigators have performed perfusion studies at 3T and have demonstrated improved SNR and contrast-to-noise ratio (CNR).[25] Recently 3D encoding methods have been combined with parallel imaging to improve spatial coverage using either 3D SSFP or 3D GRE.26

2.5 Delayed Enhancement

Images of myocardial scarring and fibrosis are obtained approximately 10–20 minutes after gadolinium administration. Images of delayed gadolinium enhancement have primarily been obtained with a breath-held segmented inversion recovery (IR) pulse sequence which has excellent contrast between normal myocardium and regions of infarction or fibrosis.27 On these images, the normal myocardium is dark and regions of infarction or scarring appear bright. More recently single-shot IR-SSFP pulse sequences have been used to obtain delayed enhancement (DE) imaging without the requirement of a breath-hold.28 However, this technique has been shown to be less accurate and has reduced contrast as compared to the IR-GRE, and thus should probably be reserved for patients who are unable to hold their breath. 29 One disadvantage of conventional IR-GRE DE imaging it that the inversion time (TI) to null normal myocardium must be chosen carefully to prevent inaccuracies in measurement of infarct size. This issue has been overcome with the development of segmented phase sensitive inversion recovery (PSIR). Phase sensitive detection enables removal of the background phase while preserving the desired sign of the magnetization during image reconstruction.30 Other recent developments include the application of free-breathing navigator 3D gradient echo pulse sequences to DE imaging31, and the application of DE imaging at 3T.32

3. Diagnostic Evaluation of Coronary Artery Disease

CMR has become an important tool for the clinical evaluation of patients with known or suspected coronary artery disease (CAD). It can assess regional and global contractile function and contractile reserve, differentiate between acute and chronic myocardial infarction (MI), evaluate myocardial ischemia and viability, and assess for the presence of microvascular obstruction (MVO), or detect left ventricular thrombus. While imaging of the coronary arteries

with CMR continues to advance, current techniques are inadequate for the routine clinical assessment of the severity of coronary artherosclerosis.

3.1 Contractile Function

Cine images of function are typically obtained in the short axis orientation covering the whole ventricle and in standard two-chamber, three-chamber, and four-chamber orientations. Regional wall motion abnormalities, cardiac chamber dimensions, myocardial mass, valvular regurgitation, and LVEF are assessed. In patients who cannot hold their breath, or have cardiac arrhythmias, real-time techniques are used to assess myocardial function.

3.2 Myocardial Edema

T2-weighted imaging, which is sensitive to myocardial edema, can help differentiate between acute and chronic MI (figure 1). In acute infarction, increases in myocardial water content due to edema lengthen T2 relaxation times resulting in increased signal intensity on T2-weighted images. In a study by Abdel-Aty et al. of 58 patients with acute or chronic MI who underwent CMR and coronary angiography, acute MI was identified by T2 weighted imaging with 91% sensitivity and 97% specificity.[33] By 30 days after the infarction the signal intensity in the region of the infarct normalized consistent with the resolution of myocardial edema in the chronic infarct.[33] Cury et al. used CMR, including T2 weighted imaging, to study 62 patients presenting to the emergency department with acute chest pain, negative biomarkers, and no ECG changes of acute ischemia. The addition of T2 weighted imaging to a protocol including function, perfusion, and DE improved the specificity, positive predictive value, and overall accuracy from 84% to 96%, 55% to 85%, and 84% to 93%, respectively, compared with the conventional CMR protocol.[34]

The region of increased T2 signal intensity has also been shown to correlate to the ischemic area at risk (the region of hypoperfusion at the time of an ischemic episode) in a canine study of transient coronary occlusion. Aletras et al. demonstrated that the region of hyperintensity on T2-weighted images corresponded in size and location to the area at risk by fluorescent microspheres in a transient coronary occlusion/reperfusion model.[35] This was larger than the region of infarction by DE imaging. The region of increased T2 at day 2 had partial recovery of function at two months consistent with viable but dysfunctional myocardium following transient ischemia.35

3.3 Assessment of Ischemia

Two methods are available for myocardial stress testing: assessment of stress-induced wall motion abnormalities using cine imaging and assessment of stress-induced perfusion abnormalities using first-pass myocardial perfusion imaging. Wall-motion analysis is primarily assessed using dobutamine infusion, but has also been performed with exercise stress.[36]

During a dobutamine stress CMR study, images of the LV are typically obtained in three long axis (2-CH, 3-CH, and 4-CH) and three short axis (base, mid, apex) orientations at baseline and at each increasing stage of dobutamine infusion ranging from 5–40 ug/kg-min. The stress study is terminated if there is a significant drop in blood pressure, development of significant arrhythmias, new wall motion abnormalities, or achievement of 85% of the age-predicted maximum heart-rate.

In a study by Nagel et al., 208 patients with suspected CAD underwent both dobutamine stress echo and dobutamine stress CMR prior to cardiac catheterization.37 With CMR, sensitivity and specificity for detecting a 50% coronary stenosis was increased from 74.3% to 86.2% and from 69.8% to 85.7% respectively compared with echocardiography. In a study of 163 patients with poor acoustic windows preventing adequate imaging by dobutamine stress echo Hundley

et al successfully performed dobutamine stress MRI in 153 of the patients.[38] The sensitivity and specificity for detecting a 50% coronary stenosis was 83% and 83% respectively in the 41 patients undergoing coronary angiography within 6 months of their stress test. In the 103 patients with negative stress tests, the event free survival at a median follow-up of 228 days was 97%. A recent meta-analysis of dobutamine stress CMR including 14 studies (754 patients) demonstrated a sensitivity of 83% (95% confidence interval [CI] 79% to 88%) and specificity of 86% (95% CI 81% to 91%).[39] The overall prevalence of CAD in this meta-analysis was 70.5%. Thus, dobutamine stress CMR is a sensitive and specific tool for diagnosis of stress-induced ischemia.

Stress perfusion images are typically obtained during infusion of 140 ug/kg/min of adenosine for 2–4 minutes while the patients HR and blood pressure are being monitored. Typically 3–4 short axis perfusion images are acquired across the left ventricle with a temporal resolution of one heart beat during the injection of 0.05–0.1 mmol/kg gadolinium contrast at a rate of 3–4 ml/s via a power injector. Forty to sixty image frames are usually obtained. After about a 10-minute period to allow for contrast washout, a second set of perfusion images using the same protocol is obtained without adenosine infusion. Images are usually evaluated visually but may also be evaluated by semi-quantitative analysis of the myocardial time-intensity curves. Absolute quantification of myocardial perfusion is also possible, but additional data must be obtained to determine the arterial input function.[40]

Adenosine stress cardiac MRI has been shown to be both sensitive and specific for detection of CAD. Figure 2 demonstrates subendocardial ischemia in a patient found to have multivessel coronary disease. A recent meta-analysis including 1516 patients with intermediate likelihood of disease (prevalence 57.4%) undergoing adenosine stress perfusion MRI demonstrated a sensitivity of 91% (95% CI 88% to 94%) and specificity of 81% (95% CI 77% to 85%).39 A recent multi-center trial of 234 patients who were studied with both single photon emission computed tomography (SPECT) and CMR perfusion imaging demonstrated superior diagnostic utility for CMR perfusion at the ideal contrast dose as compared to SPECT.41 Furthermore, multiple studies have demonstrated a good prognosis for patients with chest pain and suspected CAD who have negative CMR perfusion studies. In a study of 135 patients presenting to the emergency department with chest pain and negative troponin-I, there were no events in 107 patients without CMR perfusion abnormalities at one year, and the presence of an abnormal stress CMR was significantly predictive of major adverse cardiac events (MACE).42 In a study of 420 patients with known or suspected CAD, the presence of abnormal perfusion was associated with a 17% event rate while a normal perfusion study was associated with a 5% event rate.43 Thus CMR perfusion studies provide both diagnostic and prognostic information in patients with known or suspected coronary disease.

3.4 Assessment of Infarction and Viability

CMR using IR-DE imaging has become an important technique in the assessment and diagnosis of MI. Very close correlation between DE CMR and histopathology by TTC staining has been demonstrated by Kim et. al. in a canine model of MI.44 DE CMR has the ability to detect small subendocardial MIs which can be missed by other techniques. Wagner et al. demonstrated that CMR detects an additional 13% of subendocardial infarcts missed by SPECT.45 The prognostic importance of detecting small MIs was demonstrated by Kwong et. al. in a study of 195 patients with a clinical suspicion of coronary disease without prior clinical history of MI. After a median follow up of 16 months the presence of DE by CMR was associated with an 8 fold increase in adverse events. Even infarcts less than 2% of the ventricular volume were associated with a > 7 fold risk of MACE. In a study of 122 patients with revascularized STEMI, an infarct size by DE greater than 18.5% of the ventricle was shown to be a strong independent predictor of MACE.46 In another recent study of 231 patients with MI, Roes et al. demonstrated

that infarct size by DE CMR was a stronger predictor of all cause mortality at an average of 1.7 years of follow up than LVEF or LV volumes.[47] The presence and transmurality of DE has been shown to be predictive of functional recovery following coronary revascularization. Kim et al. demonstrated in 41 patients with chronic ischemic heart disease that dysfunctional myocardial segments with less than 25% DE were likely (>70% chance) to demonstrate functional recovery, where as segments with greater than 50% DE were unlikely (<8% chance) to improve contractile function following revascularization.[48] Choi et al. demonstrated in a study of 27 patients with acute MI, that less than 25% transmurality of DE was the best predictor of functional recovery.49 Low-dose dobutamine may also be used to evaluate for myocardial viability and may be more specific at predicting functional recovery in patients with intermediate transmurality of infarction by DE.50, 51

3.5 Evaluation of Microvascular Obstruction

CMR has the ability to demonstrate the presence of MVO in acute MI following coronary reperfusion (figure 1). MVO within a region of acute MI appears as a hypointense region within a bright infarct on heavily-T1 weighted images after contrast administration. Judd et al. demonstrated that early hypo-intense regions correlated with thioflavin-S negative regions of the infarcts on histology representing areas of no-reflow.52 In a study of 45 patients with acute MI, Wu et al. demonstrated that MVO, defined as hypoenhancement 1–2 minutes after contrast injection, was associated with a 45% rate of MACE at 16 months as compared to a 9% event rate of those without MVO.[53] Hombach et al. demonstrated in a study of 110 patients who underwent CMR after acute infarction that 46% of patients had MVO on DE images (late MVO), and MVO was an independent predictor of MACE at a mean of 225 days of follow up.[54] Nijveldt et al. showed in 60 patients with revascularized acute MI that late MVO was a stronger predictor of global and regional functional recovery at 4 months than any other angiographic, electrocardiographic, or CMR variables including transmural extent of infarction and early MVO.55

3.6 Evaluation of Left Ventricular Thrombus

Left ventricular thrombus can be detected with high sensitivity and specificity with CMR by performing a combination of post-contrast cine and DE imaging.[56–58] In a study of 361 patients with ischemic heart disease who had either surgical or pathological confirmation of left ventricular thrombus, Srichai et al. demonstrated that a combination of DE imaging and post-contrast cine imaging had a sensitivity and specificity of 88% and 99% respectively and had superior sensitivity as compared to either transthoracic or transesophageal echocardiography.[58] Recently Weinsaft et al. assessed the prevalence of ventricular thrombus in 784 patients with systolic dysfunction and found that DE imaging detected thrombus in roughly 7% of patients and was superior to pre-contrast cine imaging for detecting thrombus.[59]

4. Diagnostic Evaluation of Heart Failure / Cardiomyopathies

4.1 Diagnostic Approach

While multiple imaging techniques can evaluate ventricular function in heart failure, CMR is unique in its abilities to characterize myocardial properties such as myocardial edema, iron-overload, and scarring or fibrosis. The evaluation of heart failure utilizes a similar approach to that described above. Images of myocardial morphology can provide information about the presence and distribution of abnormal cardiac hypertrophy such as in hypertrophic cardiomyopathy, or regions of wall thinning in dilated cardiomyopathy or ischemic cardiomyopathy, or abnormalities of wall morphology in cardiac non-compaction.[60] Cine-imaging of function enables recognition of the pattern of wall motion abnormalities differentiating global from regional abnormalities, can be useful in diagnosis of the apical ballooning syndrome (ABS) [61], and enables analysis of RV dysfunction which may be a clue

to the diagnosis of arrythmogenic right ventricular cardiomyopathy. T2-weighted imaging to evaluate for myocardial edema has become a useful tool in evaluation of myocarditis, in stress-related cardiomyopathy, and in iron-overload cardiomyopathy. T2*-weighted imaging provides information about iron-content in iron-overload cardiomyopathy related to hemochromatosis or transfusion-dependent anemias. The presence and patterns of delayed gadolinium enhancement have provided new diagnostic insight into differentiating ischemic cardiomyopathy from various types of non-ischemic cardiomyopathies.62, 63 In a study by McCrohon et al., 100% of patients with depressed EF and CAD had DE in a subendocardial or transmural distribution, whereas 72% of subjects with non-ischemic cardiomyopathy had either no DE or a mid-wall distribution of DE.62 Soriano et. al. demonstrated a subendocardial or transmural distribution of DE in 81% of patients with CAD by coronary angiography but in only 9% of patients with normal coronary angiograms.[63] The presence and distribution of myocardial delayed enhancement has been shown to be a sensitive and specific tool for predicting response to chronic resynchronization therapy.[64] The absence of delayed enhancement may enable the diagnosis of the ABS in patients presenting with acute coronary syndromes and normal coronary arteries at cardiac catheterization.[65] In the following section we will review the unique diagnostic and prognostic information provided by CMR in some specific types of cardiomyopathy.

4.2 CMR in specific Cardiomyopathies

4.2.1 Dilated Cardiomyopathy—Dilated cardiomyopathy (DCM) is the third leading cause of heart failure and the leading cause of heart transplantation.[66] DCM is characterized by the presence of ventricular chamber enlargement and systolic dysfunction with normal wall thickness.66 CMR anatomical and functional imaging demonstrates reduced EF typically with global dysfunction, increased ventricular volumes, increased left-ventricular dimensions, and relative myocardial wall thinning.

CMR can be used to assess myocardial fibrosis in DCM, which has been shown to have important prognostic implications. Delayed enhancement imaging has demonstrated a distinct pattern of mid-wall ventricular scarring which occurs in roughly 30% of patients with DCM.[62] In a study of 101 consecutive DCM patients who were followed prospectively for an average of 1.8 years Assomull et. al. demonstrated that the presence of midwall fibrosis was associated with a higher rate of all-cause death and hospitalization for a cardiovascular event (HR 3.4), and was also associated with secondary outcome measures of sudden cardiac death (SCD) or ventricular tachycardia (VT) (HR 5.2).[67] Midwall-fibrosis remained predictive for SCD/VT even after adjustment for EF. Recently, a new pulse sequence for mapping T_1 relaxation after contrast administration time has demonstrated the ability to assess diffuse myocardial fibrosis, by a reduction in the T1 relaxation time. Iles et al. performed T1 mapping in 20 controls and in 25 patients with heart failure, 9 of which had endomyocardial biopsies. The post contrast T1 time was inversely correlated with histologic fibrosis (R=0.7) and was shorter than that in controls even within areas without obvious scarring by DE.[68]

4.2.2 Hypertrophic Cardiomyopathy—Hypertrophic cardiomyopathy (HCM) is an autosomal-dominant disorder characterized by mutations in one of multiple genes encoding proteins of the cardiac sarcomere.[69] It is the most common genetic cause of heart disease with an estimated incidence of 1:500 in the general population, and is the most frequent cause of SCD in young people.66 Histologically, there is disordered myocyte architecture with regions of myocardial scarring and increased collagen matrix.69

HCM is characterized by an abnormally increased wall thickness in a non-dilated ventricle in the absence of other conditions capable of producing cardiac hypertrophy such as hypertension or aortic valve stenosis.66 The diagnosis is typically made by echocardiography, but a study

of 48 patients with known or suspected HCM who underwent both CMR and echo demonstrated that echo failed to demonstrate LV hypertrophy in 6% of patients, underestimated hypertrophy in the anterolateral free wall, and underestimated the number of patients with hypertrophy greater than 3 cm in 10% of the patients.70 Furthermore, the diagnosis of apical-variant HCM can be missed by echocardiography, but correctly identified by CMR.[71] In a study of 1299 patients with HCM, 28 demonstrated apical aneurysms by CMR, but only 16 (57%) of these were detected by echocardiography.[72] Cine-imaging with CMR has also been validated for measurement of LV mass which has been shown to be a sensitive predictor for adverse outcomes.73 Furthermore, SSFP cine imaging can be used to evaluate for outflow obstruction and systolic anterior motion of the mitral valve. Myocardial tagging has also provided insight into the regional variations in myocardial function (figure 3). Despite a globally preserved EF, in many patients with HCM, regional impairment in intramyocardial deformation and increased myocardial torsion has been demonstrated.[74, 75]

As myocardial scarring is known to occur in patients with HCM, DE CMR has been applied to the detection of myocardial scarring (figure 3). Choudhury et al. studied 21 patients with known HCM who were predominantly asymptomatic with DE imaging and demonstrated myocardial scar in 81% of the patients. The scarring was predominantly patchy, multi-focal, and mid-wall within areas of hypertrophy including scarring at the junction of the interventricular septum and RV free wall.[76] Atabag et al. have investigated whether myocardial fibrosis may represent the arrythmogenic substrate in HCM. They studied 177 patients with HCM who underwent CMR with DE imaging as well as 24-hour Holter monitoring and demonstrated that patients with scarring by DE had a greater likelihood and increased frequency of PVC's, and non-sustained VT then those without scarring by DE.[77] Thus, detection of myocardial fibrosis by CMR may provide incremental information in addition to traditional risk factors for identifying patients at risk of SCD.

4.2.3 Arrythmogenic Right Ventricular Dysplasia/Cardiomyopathy— Arrythmogenic right ventricular dysplasia/cardiomyopathy (ARVD/C) is a relatively uncommon inheritable heart disease affecting predominantly the right ventricle and is characterized by progressive fibrofatty infiltration and myocyte loss resulting in right ventricular chamber enlargement, dysfunction and cardiac arrythmias that may cause SCD.[66] Demonstration of abnormalities in the RV structure and function constitutes one of the major criteria of the ARVD/C task force criteria for the diagnosis of ARVD/C.78 CMR morphologic and cine-functional imaging can provide comprehensive assessment of right ventricular dimensions, volumes, and regional and global function. One of the other major Task Force criteria is the detection of fibrofatty infiltration of the right ventricle by endomyocardial biopsy. Demonstration of fatty infiltration on CMR is a non-specific finding.79 In a multi-center study of 42 patients meeting Task-force criteria, 10 patients with idiopathic VT, and 25 controls demonstrated fatty infiltration in 60% of patients with ARVD/C, whereas RV function was abnormal in 80%, and an RV EF <50% had a sensitivity of 73% and a specificity of 95% for diagnosing AVRD/C.80

DE imaging has been applied to the evaluation of fibrosis in a study of 30 patients evaluated for possible ARVD/C. Of the 12 patients who met Task force criteria, 67% demonstrated DE in the right ventricle. The presence of DE was also correlated with histopathology and predicted inducible VT during electrophysiology studies.[81]

4.2.4 Myocarditis—Myocarditis is an acquired acute or a chronic inflammatory process of diverse etiologies which results in myocardial inflammation, edema, necrosis, and fibrosis.[66] Cine-SSFP images generally provide accurate quantification of myocardial dimensions and function (figure 4). CMR has been used to evaluate for myocardial edema. In a study of 25 patients with suspected myocarditis and 23 healthy controls, Abdel-Aty et al. demonstrated

that increased T2 signal in the myocardium had a sensitivity, specificity, and accuracy of 84%, 74%, and 79% for the diagnosis of myocarditis.[82] To evaluate for the presence of myocardial inflammation Freidrich et al. studied 44 subjects with suspected myocarditis and demonstrated an increase in the relative myocardial enhancement compared with skeletal muscle on T1 weighted TSE images obtained before and after gadolinium contrast agent administration.[83] This increased enhancement persisted for the first month after initial diagnosis, but resolved by 3 months. Abdy-Aty et al. also used the global relative enhancement in the above study and demonstrated a sensitivity, specificity, and accuracy for detecting myocarditis of 80%, 68%, and 74.5% respectively.[82]

DE imaging has been applied to evaluate fibrotic changes in myocarditis (Figure 4). In a study of 32 patients who were diagnosed with myocarditis by clinical criteria, Mahrholdt et al. used DE CMR to direct the location of myocardial biopsies. In their study DE was seen in one or multiple foci predominantly in the lateral wall in 88% of the subjects. In the 21 patients whose biopsies were taken in the region of contrast enhancement 19 patients had histopathological evidence of active myocarditis. In a study of 128 patients with suspected myocarditis, DE was present in 83 of the 87 patients with active myocarditis, and was an independent predictor of impaired ventricular function and ventricular dilation at follow up.[84] In the study by Abdel-Aty et al. the presence of DE had a sensitivity, specificity, and accuracy of 44%, 100%, and 71%, respectively.[82]

A recently published consensus document which provides recommendations for the indications, protocols and diagnostic criteria for the evaluation of myocarditis suggests that a combination of these techniques (global relative enhancement, T2, and DE) may improve the diagnostic utility of CMR.[85] The presence of abnormalities on two of the above three techniques yielded a sensitivity of 76%, a specificity of 96% and an accuracy of 85% in the study by Abdel-Aty.82

4.2.5 Sarcoid Cardiomyopathy—Sarcoidosis is a multi-system inflammatory disease of unknown etiology which is characterized pathologically by the presence of noncaseating granulomas. Symptomatic cardiac involvement occurs in up to 7% of patients, but autopsy studies estimate that greater than 25% of patients in the United States with sarcoidosis have cardiac involvement.[86] Cardiac sarcoidosis may result in arrythmias, conduction abnormalities, ventricular aneurysms, congestive heart failure and SCD.[87]

CMR has become a useful tool in the diagnostic evaluation of cardiac involvement in sarcoidosis (figure 5). Cine-functional imaging may demonstrate segmental or regional wall motion abnormalities, areas of focal wall thinning or thickening, and the presence of myocardial aneurysms. T2 weighted imaging in patients with myocardial involvement has demonstrated focal areas of increased intramyocardial signal likely as a result of granulomatous inflammation.[88, 89] CMR has been used to demonstrate myocardial scarring using DE imaging. In a study of 58 patients with biopsy-proven pulmonary sarcoidosis, CMR demonstrated a sensitivity and specificity of 100% and 78% respectively using Japanese Ministry clinical criteria as a gold standard.[90] CMR demonstrated DE in all patients who met Japanese Ministry criteria, and demonstrated DE in 6 other patients. [90]

4.2.6 Amyloid Cardiomyopathy—Amyloid is a systemic clinical disorder characterized by extracellular deposition of insoluble fibrillar proteins in multiple organ systems. Systemic AL amyloidosis, which is the most common form, affects the heart in up to 90% of patients, and in 50% of the cases the presenting symptom is heart failure.[91] Senile systemic amyloidosis has an incidence of 25–36% in those over 80 years of age and also has a high incidence of cardiac involvement.91 On functional and anatomical imaging ventricular wall thickening is commonly seen, however systolic function is generally preserved until later stages of the

disease. Patients may also have small pericardial effusions, atrial wall thickening, and valvular thickening. These features are non-specific for amyloid and can also be identified by echocardiography. Tissue characterization with CMR can provide more specific information towards the diagnosis of cardiac amyloidosis. Early studies showed a decrease in signal intensity ratio on both T1 and T2 weighted images which enabled differentiation of amyloid heart disease from hypertrophic cardiomyopathy.92 Recent studies have focused on the presence of DE. In a study of 20 patients with biopsy proven systemic amyloid and echocardiographic criteria for cardiac involvement, 69% of the patients demonstrated a pattern of diffuse subendocardial hyperenhancement, and demonstrated significantly lower T1 values after gadolinium contrast than control patients.93 Vogelsberg et. al. performed both CMR and endomyocardial biopsy in 33 consecutive patients with suspected cardiac amyloidosis. In the 15 patients with biopsy proven cardiac amyloidoisis, 12 patients demonstrated a diffuse pattern of DE by CMR which resulted in a sensitivity and specificity of 80% and 94% respectively.[94] Recently White et al. demonstrated the prognostic significance of the diffuse pattern of DE among 46 patients with histological confirmation of systemic amyloidosis and suspected cardiac involvement. In their cohort, 65% of patients demonstrated diffuse hyperenhancement on DE imaging, and this finding was associated with a median survival of 144 days (versus 600 days) and a 6 fold increase in the rate of death of heart transplantation.[95] Maceria et. al. have demonstrated that altered gadolinium kinetics in the heart which result in an abnormal intramyocardial T1 gradient predict poor prognosis in cardiac amyloidosis.96

4.2.7 Iron Overload Cardiomyopathy—Iron overload cardiomyopathy may be caused by hereditary conditions such as hemochromatosis or as a result of transfusion-dependent anemias. Heart failure is the leading cause of death, and is the cause of death in greater than 50% of Thalassemia major patients.[97] Cine imaging with SSFP pulse sequences can evaluate functional parameters such as LVEF, but reduced systolic function is a late finding in the disease. In patients with severe iron overload, the myocardium and or liver may have a darker appearance on SSFP images due to the reduced T2 and T2* which is suggestive of the diagnosis. Anderson et al studied 109 patients with Thalassemia Major with chronic transfusion therapy and 15 normal volunteers and demonstrated that the mean T2* for normal subjects was 52+/−16 ms, and below a T2* of 20ms (2 standard deviations below normal), LVEF and T2* were correlated with lower LVEF associated with lower T2* values.[98] T2* has proven to be a reproducible marker of iron overload, and has been shown to normalize in patients on chronic chelation therapy.99

5. Expert Opinion

CMR has evolved into a clinically important technique capable of performing a comprehensive evaluation of cardiac structure and function including unique information about tissue characterization. CMR has become the gold standard for quantitative evaluation of myocardial morphology and function due to its high resolution and intrinsic three-dimensional nature. While echocardiography is commonly used for evaluation of myocardial function as it is widely available and inexpensive, suboptimal images are obtained in a significant number of patients due to body habitus or lung disease. Furthermore, quantification of function by echocardiography relies on geometric assumptions and has more variability than quantification by CMR. DE CMR imaging is the most accurate cardiac imaging technique for detection and sizing of myocardial infarction and provides important prognostic information in multiple cardiovascular diseases. It has enabled detection of small subendocardial myocardial infarcts which were previously difficult to detect using conventional techniques such as SPECT, and has provided unique insight into scar patterns in various cardiomyopathies, improving the ability to differentiate etiologies of cardiomyopathies and lead to potential changes in therapy. CMR is the only cardiac imaging modality which can detect myocardial edema, or assess for myocardial iron overload. CMR is capable of performing high resolution quantitative

assessment of myocardial perfusion and perfusion reserve which is important for detecting multivessel CAD. Adding DE imaging improves its overall accuracy. CMR has significantly improved spatial resolution as compared to SPECT and is not susceptible to variable attenuation artifacts from the breasts or scattering artifacts resulting from signal in the abdominal viscera which may reduce the diagnostic accuracy of SPECT. The flexibility of CMR allows tailored imaging protocols to be used to answer specific clinical questions. As CMR does not expose patients to ionizing radiation it is ideal for longitudinal studies as well as studies assessing long term outcomes in a variety of cardiac pathologies. Given the growing concerns about increasing radiation exposure in medical imaging, this is a significant advantage over SPECT, positron emission tomography, and computed tomography.

Newer techniques involving real-time imaging and 3-D data acquisitions with parallel imaging hold promise for increased efficiency in data acquisition. These techniques are also extending the utility of CMR to patients with cardiac arrythmias and patients who are unable to hold their breath. Furthermore, the increased availability of 3 Tesla MRI scanners will provide enhanced signal which will enable new techniques to be developed, and will improve many current applications. Developments in molecular imaging agents will further extend the potential applications of CMR. Traditional contraindications to MRI such certain implantable medical devices are being overcome by advances in the design of MR-compatible medical devices.

One of the challenges for CMR, and for advanced diagnostic imaging techniques in general, is demonstrating that these techniques provide added value compared to conventional imaging modalities. This is especially important in the current healthcare environment where techniques will no longer be evaluated solely on their diagnostic utility, but will also be evaluated for cost-effectiveness. This will require large multi-center trials of different imaging techniques evaluated in head to head comparisons. As CMR techniques are still evolving, these types of studies will require standardization of CMR techniques between multiple research sites.

In summary, CMR has evolved into an extremely useful diagnostic modality in cardiovascular disease. It offers new insights into cardiac pathophysiology and aids in the diagnosis of coronary disease and the identification of the etiology of heart failure and cardiomyopathies. With expanding expertise and recognition of its diagnostic power, it will grow in importance in the armamentarium of the cardiac imager for years to come.

Acknowledgments

This work is supported by NIH grant EB003841-05 (CM Kaymer).

References

1. Stehling MK, Holzknecht NG, Laub G, Bohm D, von Smekal A, Reiser M. Single-shot T1- and T2-weighted magnetic resonance imaging of the heart with black blood: preliminary experience. MAGMA 1996 Sep–Dec;4(3–4):231–240. [PubMed: 9220412] Description of early TSE techniques for imaging the heart
2. Vignaux OB, Augui J, Coste J, Argaud C, Le Roux P, Carlier PG, et al. Comparison of single-shot fast spin-echo and conventional spin-echo sequences for MR imaging of the heart: initial experience. Radiology 2001 May;219(2):545–550. [PubMed: 11323486]
3. Carr JC, Simonetti O, Bundy J, Li D, Pereles S, Finn JP. Cine MR angiography of the heart with segmented true fast imaging with steady-state precession. Radiology 2001 Jun;219(3):828–834. [PubMed: 11376278] Description of the application of SSFP pulse sequences to imaging the heart
4. Fieno DS, Jaffe WC, Simonetti OP, Judd RM, Finn JP. TrueFISP: assessment of accuracy for measurement of left ventricular mass in an animal model. J Magn Reson Imaging 2002 May;15(5): 526–531. [PubMed: 11997893]

5. Lorenz CH, Walker ES, Morgan VL, Klein SS, Graham TP Jr. Normal human right and left ventricular mass, systolic function, and gender differences by cine magnetic resonance imaging. J Cardiovasc Magn Reson 1999;1(1):7–21. [PubMed: 11550343]
6. Wintersperger BJ, Nikolaou K, Dietrich O, Rieber J, Nittka M, Reiser MF, et al. Single breath-hold real-time cine MR imaging: improved temporal resolution using generalized autocalibrating partially parallel acquisition (GRAPPA) algorithm. Eur Radiol 2003 Aug;13(8):1931–1936. [PubMed: 12783177]
7. Lee VS, Resnick D, Bundy JM, Simonetti OP, Lee P, Weinreb JC. Cardiac function: MR evaluation in one breath hold with real-time true fast imaging with steady-state precession. Radiology 2002 Mar; 222(3):835–842. [PubMed: 11867810] Real-time SSFP imaging of the heart
8. Mascarenhas NB, Muthupillai R, Cheong B, Pereyra M, Flamm SD. Fast 3D cine steady-state free precession imaging with sensitivity encoding for assessment of left ventricular function in a single breath-hold. AJR Am J Roentgenol 2006 Nov;187(5):1235–1239. [PubMed: 17056910]
9. Axel L, Dougherty L. MR imaging of motion with spatial modulation of magnetization. Radiology 1989 Jun;171(3):841–845. [PubMed: 2717762] Original description of SPAMM myocardial tagging
10. Aletras AH, Ding S, Balaban RS, Wen H. DENSE: displacement encoding with stimulated echoes in cardiac functional MRI. J Magn Reson 1999 Mar;137(1):247–252. [PubMed: 10053155] First description of DENSE phase tagging for assessing myocardial strain
11. Kim D, Gilson WD, Kramer CM. Epstein FH. Myocardial tissue tracking with two-dimensional cine displacement-encoded MR imaging: development and initial evaluation. Radiology 2004 Mar;230 (3):862–871. [PubMed: 14739307]
12. Osman NF, Kerwin WS, McVeigh ER, Prince JL. Cardiac motion tracking using CINE harmonic phase (HARP) magnetic resonance imaging. Magn Reson Med 1999 Dec;42(6):1048–1060. [PubMed: 10571926] Original description of the HARP technique for cardiac motion tracking
13. Simonetti OP, Finn JP, White RD, Laub G, Henry DA. "Black blood" T2-weighted inversion-recovery MR imaging of the heart. Radiology 1996 Apr;199(1):49–57. [PubMed: 8633172] Description of Double-Inversion Black-Blood T2 weighted imaging
14. Kellman P, Aletras AH, Mancini C, McVeigh ER, Arai AE. T2-prepared SSFP improves diagnostic confidence in edema imaging in acute myocardial infarction compared to turbo spin echo. Magn Reson Med 2007 May;57(5):891–897. [PubMed: 17457880]
15. Aletras AH, Kellman P, Derbyshire JA, Arai AE. ACUT2E TSE-SSFP: a hybrid method for T2-weighted imaging of edema in the heart. Magn Reson Med 2008 Feb;59(2):229–235. [PubMed: 18228588]
16. Pepe A, Positano V, Santarelli MF, Sorrentino F, Cracolici E, De Marchi D, et al. Multislice multiecho T2* cardiovascular magnetic resonance for detection of the heterogeneous distribution of myocardial iron overload. J Magn Reson Imaging 2006 May;23(5):662–668. [PubMed: 16568436] Multi-slice T2* weighted pulse sequence description for evaluation of iron overload
17. He T, Gatehouse PD, Anderson LJ, Tanner M, Keegan J, Pennell DJ, et al. Development of a novel optimized breathhold technique for myocardial T2 measurement in thalassemia. J Magn Reson Imaging 2006 Sep;24(3):580–585. [PubMed: 16892203]
18. Kellman P, Arai AE. Imaging sequences for first pass perfusion --a review. J Cardiovasc Magn Reson 2007;9(3):525–537. [PubMed: 17365232] Recent review of CMR perfusion pulse sequences
19. Atkinson DJ, Burstein D, Edelman RR. First-pass cardiac perfusion: evaluation with ultrafast MR imaging. Radiology 1990 Mar;174(3 Pt 1):757–762. [PubMed: 2305058] Orignial description of contrast enhanced perfusion imaging of the heart
20. Epstein FH, Arai AE. Optimization of fast cardiac imaging using an echo-train readout. J Magn Reson Imaging 2000 Feb;11(2):75–80. [PubMed: 10713937]
21. Schreiber WG, Schmitt M, Kalden P, Mohrs OK, Kreitner KF, Thelen M. Dynamic contrast-enhanced myocardial perfusion imaging using saturation-prepared TrueFISP. J Magn Reson Imaging 2002 Dec;16(6):641–652. [PubMed: 12451577]
22. Kellman P, Derbyshire JA, Agyeman KO, McVeigh ER, Arai AE. Extended coverage first-pass perfusion imaging using slice-interleaved TSENSE. Magn Reson Med 2004 Jan;51(1):200–204. [PubMed: 14705062]

23. Fenchel M, Helber U, Simonetti OP, Stauder NI, Kramer U, Nguyen CN, et al. Multislice first-pass myocardial perfusion imaging: Comparison of saturation recovery (SR)-TrueFISP-two-dimensional (2D) and SR-TurboFLASH-2D pulse sequences. J Magn Reson Imaging 2004 May;19(5):555–563. [PubMed: 15112304]
24. Weber S, Kronfeld A, Kunz RP, Fiebich M, Horstick G, Kreitner KF, et al. Comparison of three accelerated pulse sequences for semiquantitative myocardial perfusion imaging using sensitivity encoding incorporating temporal filtering (TSENSE). J Magn Reson Imaging 2007 Sep;26(3):569–579. [PubMed: 17685447]
25. Araoz PA, Glockner JF, McGee KP, Potter DD Jr, Valeti VU, Stanley DW, et al. 3 Tesla MR imaging provides improved contrast in first-pass myocardial perfusion imaging over a range of gadolinium doses. J Cardiovasc Magn Reson 2005;7(3):559–564. [PubMed: 15959968]
26. Shin T, Hu HH, Pohost GM, Nayak KS. Three dimensional first-pass myocardial perfusion imaging at 3T: feasibility study. J Cardiovasc Magn Reson 2008;10(1):57. [PubMed: 19077220]
27. Simonetti OP, Kim RJ, Fieno DS, Hillenbrand HB, Wu E, Bundy JM, et al. An improved MR imaging technique for the visualization of myocardial infarction. Radiology 2001 Jan;218(1):215–223. [PubMed: 11152805] Key reference describing delayed enhancement pulse sequence
28. Li W, Li BS, Polzin JA, Mai VM, Prasad PV, Edelman RR. Myocardial delayed enhancement imaging using inversion recovery single-shot steady-state free precession: initial experience. J Magn Reson Imaging 2004 Aug;20(2):327–330. [PubMed: 15269961]
29. Sievers B, Elliott MD, Hurwitz LM, Albert TS, Klem I, Rehwald WG, et al. Rapid detection of myocardial infarction by subsecond, free-breathing delayed contrast-enhancement cardiovascular magnetic resonance. Circulation 2007 Jan 16;115(2):236–244. [PubMed: 17200443]
30. Kellman P, Arai AE, McVeigh ER, Aletras AH. Phase-sensitive inversion recovery for detecting myocardial infarction using gadolinium-delayed hyperenhancement. Magn Reson Med 2002 Feb;47 (2):372–383. [PubMed: 11810682] Description of the application of phase sensitive detection to overcome limitations of original delayed ehnancement technique
31. Nguyen TD, Spincemaille P, Weinsaft JW, Ho BY, Cham MD, Prince MR, et al. A fast navigator-gated 3D sequence for delayed enhancement MRI of the myocardium: comparison with breathhold 2D imaging. J Magn Reson Imaging 2008 Apr;27(4):802–808. [PubMed: 18302233]
32. Klumpp B, Fenchel M, Hoevelborn T, Helber U, Scheule A, Claussen C, et al. Assessment of myocardial viability using delayed enhancement magnetic resonance imaging at 3.0 Tesla. Invest Radiol 2006 Sep;41(9):661–667. [PubMed: 16896300]
33. Abdel-Aty H, Zagrosek A, Schulz-Menger J, Taylor AJ, Messroghli D, Kumar A, et al. Delayed enhancement and T2-weighted cardiovascular magnetic resonance imaging differentiate acute from chronic myocardial infarction. Circulation 2004 May 25;109(20):2411–2416. [PubMed: 15123531] Clinical application of T2-weighted imaging for acute myocardial infarction
34. Cury RC, Shash K, Nagurney JT, Rosito G, Shapiro MD, Nomura CH, et al. Cardiac magnetic resonance with T2-weighted imaging improves detection of patients with acute coronary syndrome in the emergency department. Circulation 2008 Aug 19;118(8):837–844. [PubMed: 18678772]
35. Aletras AH, Tilak GS, Natanzon A, Hsu LY, Gonzalez FM, Hoyt RF Jr, et al. Retrospective determination of the area at risk for reperfused acute myocardial infarction with T2-weighted cardiac magnetic resonance imaging: histopathological and displacement encoding with stimulated echoes (DENSE) functional validations. Circulation 2006 Apr 18;113(15):1865–1870. [PubMed: 16606793] Animal study showing link between T2 and ischemic area at risk
36. Rerkpattanapipat P, Gandhi SK, Darty SN, Williams RT, Davis AD, Mazur W, et al. Feasibility to detect severe coronary artery stenoses with upright treadmill exercise magnetic resonance imaging. Am J Cardiol 2003 Sep 1;92(5):603–606. [PubMed: 12943887]
37. Nagel E, Lehmkuhl HB, Bocksch W, Klein C, Vogel U, Frantz E, et al. Noninvasive diagnosis of ischemia-induced wall motion abnormalities with the use of high-dose dobutamine stress MRI: comparison with dobutamine stress echocardiography. Circulation 1999 Feb 16;99(6):763–770. [PubMed: 9989961] Large clinical study of dobutamine CMR stress testing
38. Hundley WG, Hamilton CA, Thomas MS, Herrington DM, Salido TB, Kitzman DW, et al. Utility of fast cine magnetic resonance imaging and display for the detection of myocardial ischemia in patients not well suited for second harmonic stress echocardiography. Circulation 1999 Oct 19;100(16):1697–1702. [PubMed: 10525488]

39. Nandalur KR, Dwamena BA, Choudhri AF, Nandalur MR, Carlos RC. Diagnostic performance of stress cardiac magnetic resonance imaging in the detection of coronary artery disease: a meta-analysis. J Am Coll Cardiol 2007 Oct 2;50(14):1343–1353. [PubMed: 17903634] Recent meta-analysis of both perfusion and dobutamine stress CMR
40. Wilke N, Jerosch-Herold M, Wang Y, Huang Y, Christensen BV, Stillman AE, et al. Myocardial perfusion reserve: assessment with multisection, quantitative, first-pass MR imaging. Radiology 1997 Aug;204(2):373–384. [PubMed: 9240523]
41. Schwitter J, Wacker CM, van Rossum AC, Lombardi M, Al-Saadi N, Ahlstrom H, et al. MR-IMPACT: comparison of perfusion-cardiac magnetic resonance with single-photon emission computed tomography for the detection of coronary artery disease in a multicentre, multivendor, randomized trial. Eur Heart J 2008 Feb;29(4):480–489. [PubMed: 18208849]
42. Ingkanisorn WP, Kwong RY, Bohme NS, Geller NL, Rhoads KL, Dyke CK, et al. Prognosis of negative adenosine stress magnetic resonance in patients presenting to an emergency department with chest pain. J Am Coll Cardiol 2006 Apr 4;47(7):1427–1432. [PubMed: 16580532]
43. Bodi V, Sanchis J, Lopez-Lereu MP, Nunez J, Mainar L, Monmeneu JV, et al. Prognostic value of dipyridamole stress cardiovascular magnetic resonance imaging in patients with known or suspected coronary artery disease. J Am Coll Cardiol 2007 Sep 18;50(12):1174–1179. [PubMed: 17868810]
44. Kim RJ, Fieno DS, Parrish TB, Harris K, Chen EL, Simonetti O, et al. Relationship of MRI delayed contrast enhancement to irreversible injury, infarct age, and contractile function. Circulation 1999;100(19):1992–2002. [PubMed: 10556226]
45. Wagner A, Mahrholdt H, Holly TA, Elliott MD, Regenfus M, Parker M, et al. Contrast-enhanced MRI and routine single photon emission computed tomography (SPECT) perfusion imaging for detection of subendocardial myocardial infarcts: an imaging study. Lancet 2003 Feb 1;361(9355): 374–379. [PubMed: 12573373] Important article demonstrating increased ability to detect myocardial infarction by CMR as compared to SPECT
46. Wu E, Ortiz JT, Tejedor P, Lee DC, Bucciarelli-Ducci C, Kansal P, et al. Infarct size by contrast enhanced cardiac magnetic resonance is a stronger predictor of outcomes than left ventricular ejection fraction or end-systolic volume index: prospective cohort study. Heart 2008 Jun;94(6):730–736. [PubMed: 18070953]
47. Roes SD, Kelle S, Kaandorp TA, Kokocinski T, Poldermans D, Lamb HJ, et al. Comparison of myocardial infarct size assessed with contrast-enhanced magnetic resonance imaging and left ventricular function and volumes to predict mortality in patients with healed myocardial infarction. Am J Cardiol 2007 Sep 15;100(6):930–936. [PubMed: 17826372]
48. Kim RJ, Wu E, Rafael A, Chen EL, Parker MA, Simonetti O, et al. The use of contrast-enhanced magnetic resonance imaging to identify reversible myocardial dysfunction. N Engl J Med 2000 Nov 16;343(20):1445–1453. [PubMed: 11078769] Important article describing the prediction of functional recovery with delayed enhancement CMR
49. Choi KM, Kim RJ, Gubernikoff G, Vargas JD, Parker M, Judd RM. Transmural extent of acute myocardial infarction predicts long-term improvement in contractile function. Circulation 2001 Sep 4;104(10):1101–1107. [PubMed: 11535563]
50. Bove CM, DiMaria JM, Voros S, Conaway MR, Kramer CM. Dobutamine response and myocardial infarct transmurality: functional improvement after coronary artery bypass grafting--initial experience. Radiology 2006 Sep;240(3):835–841. [PubMed: 16926330]
51. Wellnhofer E, Olariu A, Klein C, Grafe M, Wahl A, Fleck E, et al. Magnetic resonance low-dose dobutamine test is superior to SCAR quantification for the prediction of functional recovery. Circulation 2004 May 11;109(18):2172–2174. [PubMed: 15117834]
52. Judd RM, Lugo-Olivieri CH, Arai M, Kondo T, Croisille P, Lima JA, et al. Physiological basis of myocardial contrast enhancement in fast magnetic resonance images of 2-day-old reperfused canine infarcts. Circulation 1995 Oct 1;92(7):1902–1910. [PubMed: 7671375] Description of CMR in acute infarct including detection of MVO
53. Wu XS, Ewert DL, Liu YH, Ritman EL. In vivo relation of intramyocardial blood volume to myocardial perfusion. Evidence supporting microvascular site for autoregulation. Circulation 1992 Feb;85(2):730–737. [PubMed: 1735165]
54. Hombach V, Grebe O, Merkle N, Waldenmaier S, Hoher M, Kochs M, et al. Sequelae of acute myocardial infarction regarding cardiac structure and function and their prognostic significance as

assessed by magnetic resonance imaging. Eur Heart J 2005 Mar;26(6):549–557. [PubMed: 15713695]

55. Nijveldt R, Beek AM, Hirsch A, Stoel MG, Hofman MB, Umans VA, et al. Functional recovery after acute myocardial infarction: comparison between angiography, electrocardiography, and cardiovascular magnetic resonance measures of microvascular injury. J Am Coll Cardiol 2008 Jul 15;52(3):181–189. [PubMed: 18617066]
56. Barkhausen J, Hunold P, Eggebrecht H, Schuler WO, Sabin GV, Erbel R, et al. Detection and characterization of intracardiac thrombi on MR imaging. AJR Am J Roentgenol 2002 Dec;179(6): 1539–1544. [PubMed: 12438051]
57. Mollet NR, Dymarkowski S, Volders W, Wathiong J, Herbots L, Rademakers FE, et al. Visualization of ventricular thrombi with contrast-enhanced magnetic resonance imaging in patients with ischemic heart disease. Circulation 2002 Dec 3;106(23):2873–2876. [PubMed: 12460863]
58. Srichai MB, Junor C, Rodriguez LL, Stillman AE, Grimm RA, Lieber ML, et al. Clinical, imaging, and pathological characteristics of left ventricular thrombus: a comparison of contrast-enhanced magnetic resonance imaging, transthoracic echocardiography, and transesophageal echocardiography with surgical or pathological validation. Am Heart J 2006 Jul;152(1):75–84. [PubMed: 16824834] Comparative study for using CMR to detect LV thrombus
59. Weinsaft JW, Kim HW, Shah DJ, Klem I, Crowley AL, Brosnan R, et al. Detection of left ventricular thrombus by delayed-enhancement cardiovascular magnetic resonance prevalence and markers in patients with systolic dysfunction. J Am Coll Cardiol 2008 Jul 8;52(2):148–157. [PubMed: 18598895]
60. Petersen SE, Selvanayagam JB, Wiesmann F, Robson MD, Francis JM, Anderson RH, et al. Left ventricular non-compaction: insights from cardiovascular magnetic resonance imaging. J Am Coll Cardiol 2005 Jul 5;46(1):101–105. [PubMed: 15992642]
61. Mitchell JH, Hadden TB, Wilson JM, Achari A, Muthupillai R, Flamm SD. Clinical features and usefulness of cardiac magnetic resonance imaging in assessing myocardial viability and prognosis in Takotsubo cardiomyopathy (transient left ventricular apical ballooning syndrome). Am J Cardiol 2007 Jul 15;100(2):296–301. [PubMed: 17631086]
62. McCrohon JA, Moon JC, Prasad SK, McKenna WJ, Lorenz CH, Coats AJ, et al. Differentiation of heart failure related to dilated cardiomyopathy and coronary artery disease using gadolinium-enhanced cardiovascular magnetic resonance. Circulation 2003 Jul 8;108(1):54–59. [PubMed: 12821550] Key paper in differentiation between ischemic and non-ischemic cardiomyopathy
63. Soriano CJ, Ridocci F, Estornell J, Jimenez J, Martinez V, De Velasco JA. Noninvasive diagnosis of coronary artery disease in patients with heart failure and systolic dysfunction of uncertain etiology, using late gadolinium-enhanced cardiovascular magnetic resonance. J Am Coll Cardiol 2005 Mar 1;45(5):743–748. [PubMed: 15734620]
64. White JA, Yee R, Yuan X, Krahn A, Skanes A, Parker M, et al. Delayed enhancement magnetic resonance imaging predicts response to cardiac resynchronization therapy in patients with intraventricular dyssynchrony. J Am Coll Cardiol 2006 Nov 21;48(10):1953–1960. [PubMed: 17112984]
65. Eitel I, Behrendt F, Schindler K, Kivelitz D, Gutberlet M, Schuler G, et al. Differential diagnosis of suspected apical ballooning syndrome using contrast-enhanced magnetic resonance imaging. Eur Heart J 2008 Nov;29(21):2651–2659. [PubMed: 18820322]
66. Maron BJ, Towbin JA, Thiene G, Antzelevitch C, Corrado D, Arnett D, et al. Contemporary definitions and classification of the cardiomyopathies: an American Heart Association Scientific Statement from the Council on Clinical Cardiology, Heart Failure and Transplantation Committee; Quality of Care and Outcomes Research and Functional Genomics and Translational Biology Interdisciplinary Working Groups; and Council on Epidemiology and Prevention. Circulation 2006 Apr 11;113(14):1807–1816. [PubMed: 16567565]
67. Assomull RG, Prasad SK, Lyne J, Smith G, Burman ED, Khan M, et al. Cardiovascular magnetic resonance, fibrosis, and prognosis in dilated cardiomyopathy. J Am Coll Cardiol 2006 Nov 21;48 (10):1977–1985. [PubMed: 17112987]
68. Iles L, Pfluger H, Phrommintikul A, Cherayath J, Aksit P, Gupta SN, et al. Evaluation of diffuse myocardial fibrosis in heart failure with cardiac magnetic resonance contrast-enhanced T1 mapping. J Am Coll Cardiol 2008 Nov 4;52(19):1574–1580. [PubMed: 19007595]

69. Maron BJ. Hypertrophic cardiomyopathy: a systematic review. JAMA 2002 Mar 13;287(10):1308–1320. [PubMed: 11886323]
70. Rickers C, Wilke NM, Jerosch-Herold M, Casey SA, Panse P, Panse N, et al. Utility of cardiac magnetic resonance imaging in the diagnosis of hypertrophic cardiomyopathy. Circulation 2005 Aug 9;112(6):855–861. [PubMed: 16087809] Utility of CMR in the diagnosis of HCM
71. Moon JC, Fisher NG, McKenna WJ, Pennell DJ. Detection of apical hypertrophic cardiomyopathy by cardiovascular magnetic resonance in patients with non-diagnostic echocardiography. Heart 2004 Jun;90(6):645–649. [PubMed: 15145868]
72. Maron MS, Finley JJ, Bos JM, Hauser TH, Manning WJ, Haas TS, et al. Prevalence, clinical significance, and natural history of left ventricular apical aneurysms in hypertrophic cardiomyopathy. Circulation 2008 Oct 7;118(15):1541–1549. [PubMed: 18809796]
73. Olivotto I, Maron MS, Autore C, Lesser JR, Rega L, Casolo G, et al. Assessment and significance of left ventricular mass by cardiovascular magnetic resonance in hypertrophic cardiomyopathy. J Am Coll Cardiol 2008 Aug 12;52(7):559–566. [PubMed: 18687251]
74. Young AA, Kramer CM, Ferrari VA, Axel L, Reichek N. Three-dimensional left ventricular deformation in hypertrophic cardiomyopathy. Circulation 1994 Aug;90(2):854–867. [PubMed: 8044957]
75. Kramer CM, Reichek N, Ferrari VA, Theobald T, Dawson J, Axel L. Regional heterogeneity of function in hypertrophic cardiomyopathy. Circulation 1994 Jul;90(1):186–194. [PubMed: 8025995]
76. Choudhury L, Mahrholdt H, Wagner A, Choi KM, Elliott MD, Klocke FJ, et al. Myocardial scarring in asymptomatic or mildly symptomatic patients with hypertrophic cardiomyopathy. J Am Coll Cardiol 2002 Dec 18;40(12):2156–2164. [PubMed: 12505229] Application of delayed enhancement imaging in HCM
77. Adabag AS, Maron BJ, Appelbaum E, Harrigan CJ, Buros JL, Gibson CM, et al. Occurrence and frequency of arrhythmias in hypertrophic cardiomyopathy in relation to delayed enhancement on cardiovascular magnetic resonance. J Am Coll Cardiol 2008 Apr 8;51(14):1369–1374. [PubMed: 18387438]
78. McKenna WJ, Thiene G, Nava A, Fontaliran F, Blomstrom-Lundqvist C, Fontaine G, et al. Diagnosis of arrhythmogenic right ventricular dysplasia/cardiomyopathy. Task Force of the Working Group Myocardial and Pericardial Disease of the European Society of Cardiology and of the Scientific Council on Cardiomyopathies of the International Society and Federation of Cardiology. Br Heart J 1994 Mar;71(3):215–218. [PubMed: 8142187]
79. Tandri H, Castillo E, Ferrari VA, Nasir K, Dalal D, Bomma C, et al. Magnetic resonance imaging of arrhythmogenic right ventricular dysplasia: sensitivity, specificity, and observer variability of fat detection versus functional analysis of the right ventricle. J Am Coll Cardiol 2006 Dec 5;48(11):2277–2284. [PubMed: 17161260] Utility of CMR techniques for diagnosis of ARVD/C
80. Tandri H, Macedo R, Calkins H, Marcus F, Cannom D, Scheinman M, et al. Role of magnetic resonance imaging in arrhythmogenic right ventricular dysplasia: insights from the North American arrhythmogenic right ventricular dysplasia (ARVD/C) study. Am Heart J 2008 Jan;155(1):147–153. [PubMed: 18082506]
81. Tandri H, Saranathan M, Rodriguez ER, Martinez C, Bomma C, Nasir K, et al. Noninvasive detection of myocardial fibrosis in arrhythmogenic right ventricular cardiomyopathy using delayed-enhancement magnetic resonance imaging. J Am Coll Cardiol 2005 Jan 4;45(1):98–103. [PubMed: 15629382]
82. Abdel-Aty H, Boye P, Zagrosek A, Wassmuth R, Kumar A, Messroghli D, et al. Diagnostic performance of cardiovascular magnetic resonance in patients with suspected acute myocarditis: comparison of different approaches. J Am Coll Cardiol 2005 Jun 7;45(11):1815–1822. [PubMed: 15936612]
83. Friedrich MG, Strohm O, Schulz-Menger J, Marciniak H, Luft FC, Dietz R. Contrast media-enhanced magnetic resonance imaging visualizes myocardial changes in the course of viral myocarditis. Circulation 1998 May 12;97(18):1802–1809. [PubMed: 9603535]
84. Mahrholdt H, Wagner A, Deluigi CC, Kispert E, Hager S, Meinhardt G, et al. Presentation, patterns of myocardial damage, and clinical course of viral myocarditis. Circulation 2006 Oct 10;114(15):1581–1590. [PubMed: 17015795] Use of delayed enhancement for the diagnosis of myocarditis

85. Friedrich MG, Sechtem U, Schulz-Menger J, Holmvang G, Alakija P, Cooper LT, et al. Cardiovascular magnetic resonance in myocarditis: A JACC White Paper. J Am Coll Cardiol 2009 Apr 28;53(17):1475–1487. [PubMed: 19389557] Consensus statement concerning the use of CMR for the diagnosis of myocarditis
86. Kim JS, Judson MA, Donnino R, Gold M, Cooper LT Jr, Prystowsky EN, et al. Cardiac sarcoidosis. Am Heart J 2009 Jan;157(1):9–21. [PubMed: 19081391]
87. Sharma OP, Maheshwari A, Thaker K. Myocardial sarcoidosis. Chest 1993 Jan;103(1):253–258. [PubMed: 8417889]
88. Vignaux O. Cardiac sarcoidosis: spectrum of MRI features. AJR Am J Roentgenol 2005 Jan;184(1): 249–254. [PubMed: 15615984]
89. Vignaux O, Dhote R, Duboc D, Blanche P, Devaux JY, Weber S, et al. Detection of myocardial involvement in patients with sarcoidosis applying T2-weighted, contrast-enhanced, and cine magnetic resonance imaging: initial results of a prospective study. J Comput Assist Tomogr 2002 Sep–Oct;26(5):762–767. [PubMed: 12439312] Utility of CMR techniques in Sarcoidosis
90. Smedema JP, Snoep G, van Kroonenburgh MP, van Geuns RJ, Dassen WR, Gorgels AP, et al. Evaluation of the accuracy of gadolinium-enhanced cardiovascular magnetic resonance in the diagnosis of cardiac sarcoidosis. J Am Coll Cardiol 2005 May 17;45(10):1683–1690. [PubMed: 15893188]
91. Selvanayagam JB, Hawkins PN, Paul B, Myerson SG, Neubauer S. Evaluation and management of the cardiac amyloidosis. J Am Coll Cardiol 2007 Nov 27;50(22):2101–2110. [PubMed: 18036445]
92. Fattori R, Rocchi G, Celletti F, Bertaccini P, Rapezzi C, Gavelli G. Contribution of magnetic resonance imaging in the differential diagnosis of cardiac amyloidosis and symmetric hypertrophic cardiomyopathy. Am Heart J 1998 Nov;136(5):824–830. [PubMed: 9812077]
93. Maceira AM, Joshi J, Prasad SK, Moon JC, Perugini E, Harding I, et al. Cardiovascular magnetic resonance in cardiac amyloidosis. Circulation 2005 Jan 18;111(2):186–193. [PubMed: 15630027] Description of diffuse pattern of delayed enhancement in cardiac amyloidosis
94. Vogelsberg H, Mahrholdt H, Deluigi CC, Yilmaz A, Kispert EM, Greulich S, et al. Cardiovascular magnetic resonance in clinically suspected cardiac amyloidosis: noninvasive imaging compared to endomyocardial biopsy. J Am Coll Cardiol 2008 Mar 11;51(10):1022–1030. [PubMed: 18325442]
95. White JA, Patel MR. The role of cardiovascular MRI in heart failure and the cardiomyopathies. Cardiol Clin 2007 Feb;25(1):71–95. vi. [PubMed: 17478241]
96. Maceira AM, Prasad SK, Hawkins PN, Roughton M, Pennell DJ. Cardiovascular magnetic resonance and prognosis in cardiac amyloidosis. J Cardiovasc Magn Reson 2008;10(1):54. [PubMed: 19032744]
97. Borgna-Pignatti C, Cappellini MD, De Stefano P, Del Vecchio GC, Forni GL, Gamberini MR, et al. Survival and complications in thalassemia. Ann N Y Acad Sci 2005;1054:40–47. [PubMed: 16339650]
98. Anderson LJ, Holden S, Davis B, Prescott E, Charrier CC, Bunce NH, et al. Cardiovascular T2-star (T2*) magnetic resonance for the early diagnosis of myocardial iron overload. Eur Heart J 2001 Dec; 22(23):2171–2179. [PubMed: 11913479] Description of pulse sequence for measuring iron overload with T2*
99. Tanner MA, Galanello R, Dessi C, Smith GC, Westwood MA, Agus A. A randomized, placebo-controlled, double-blind trial of the effect of combined therapy with deferoxamine and deferiprone on myocardial iron in thalassemia major using cardiovascular magnetic resonance. Circulation 2007 Apr 10;115(14):1876–1884. [PubMed: 17372174] CMR and treatment of iron-overload cardiomyopathy

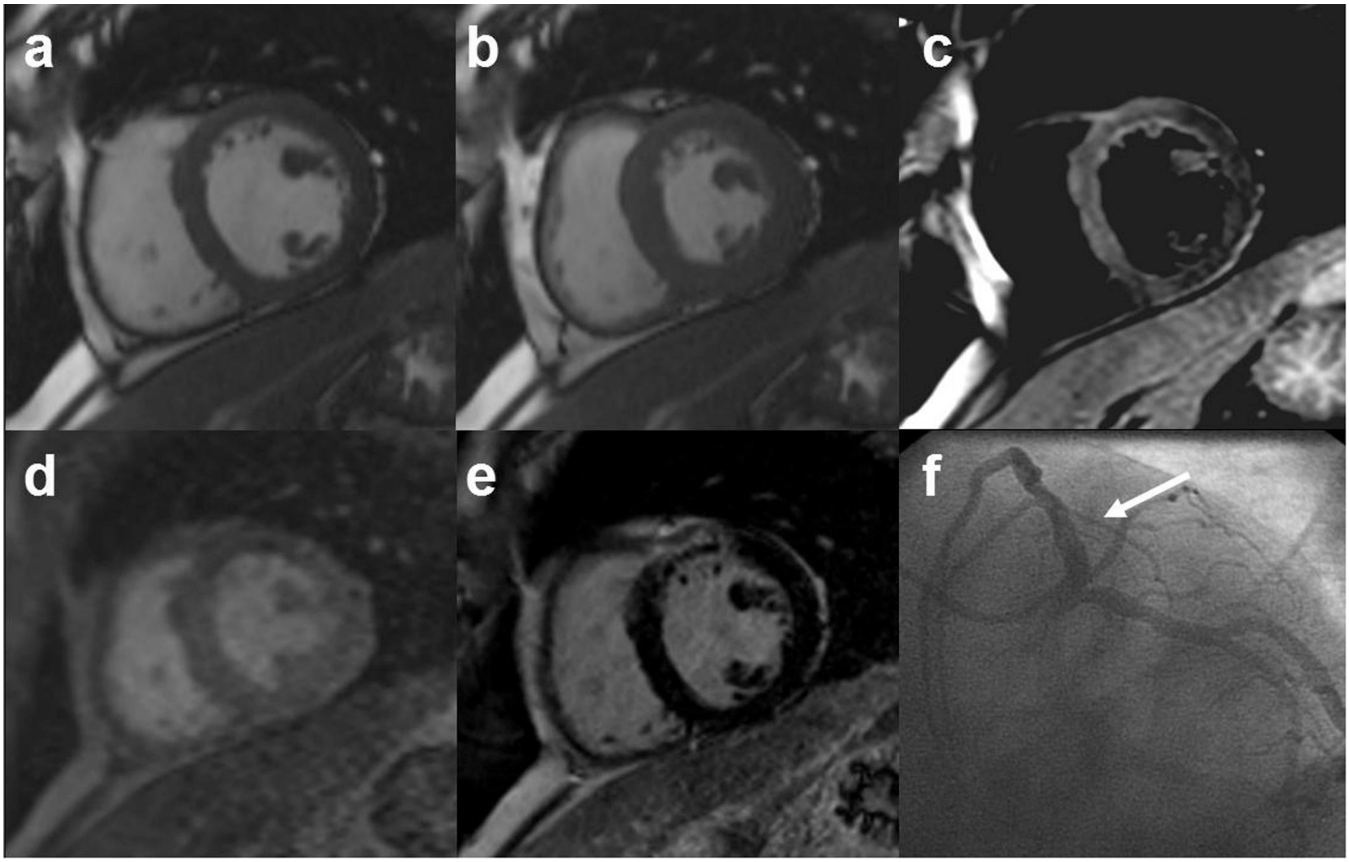

Figure 1.
CMR images from a 46 yo M with diabetes and chest pain. Cine SSFP images at (a) end diastole and (b) end systole demonstrate a focal wall motion abnormality in the anteroseptum. (c) T2-weighted TSE images demonstrate acute edema in the septum and anterior wall. (d) first pass perfusion image shows a region of hypoperfusion in the anteroseptum. (e) delayed enhancement image demonstrates a myocardial infarction with a large area of MVO. These findings were consistent with an acute myocardial infarction in a diagonal branch which was originally missed on (f) cardiac catheterization.

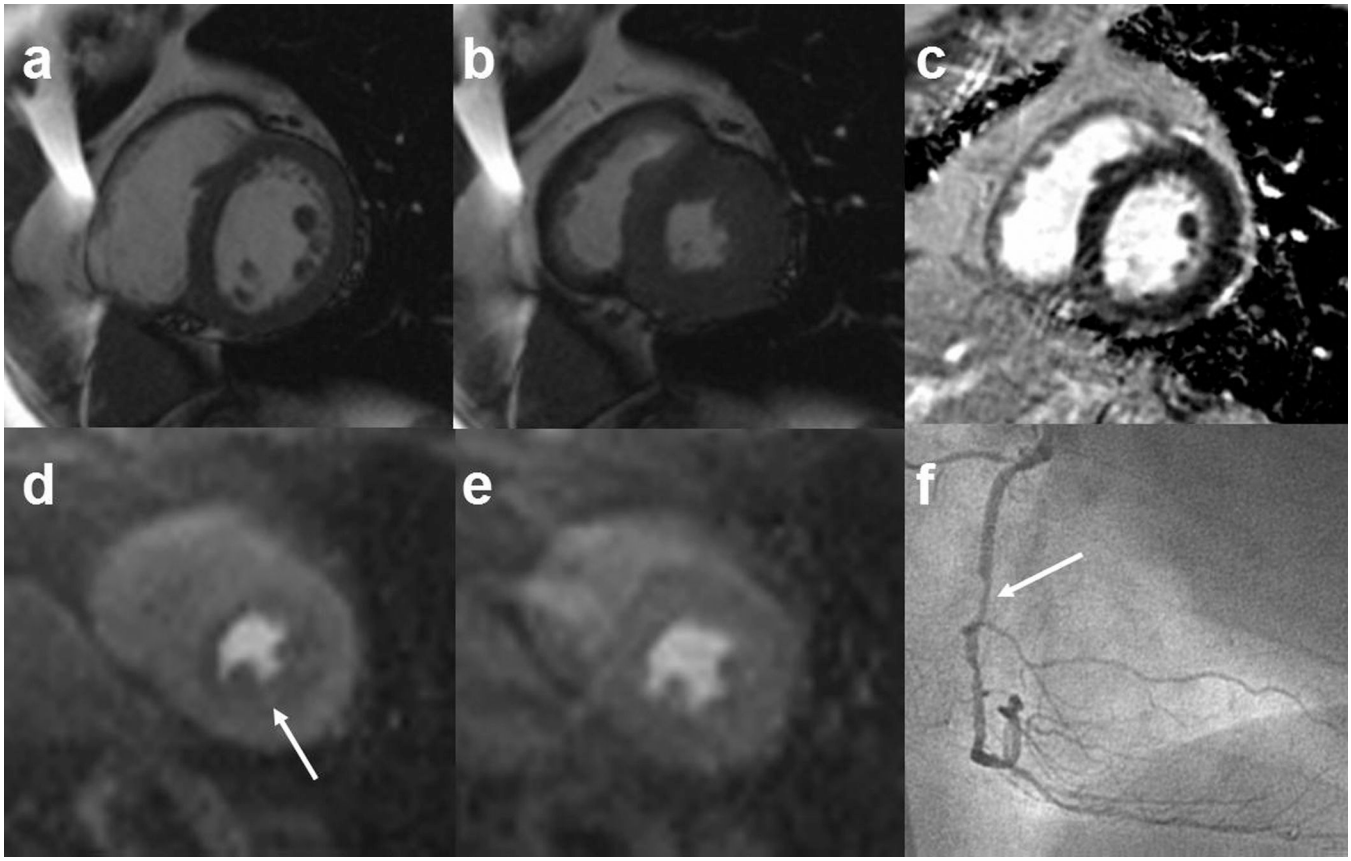

Figure 2.
CMR images from a 54yo M with diabetes and chest pain. Cine SSFP images at (a) end diastole and (b) end systole demonstrate normal wall motion. Perfusion images at stress (d) demonstrate subendocardial hypoperfusion in multiple territories which are not seen at (e) rest consistent with inducible ischemia. (c) PSIR image does not demonstrate evidence of myocardial infarction. Coronary angiography demonstrated significant stenoses in the (f) RCA and LCx and diffuse disease in the LAD territory.

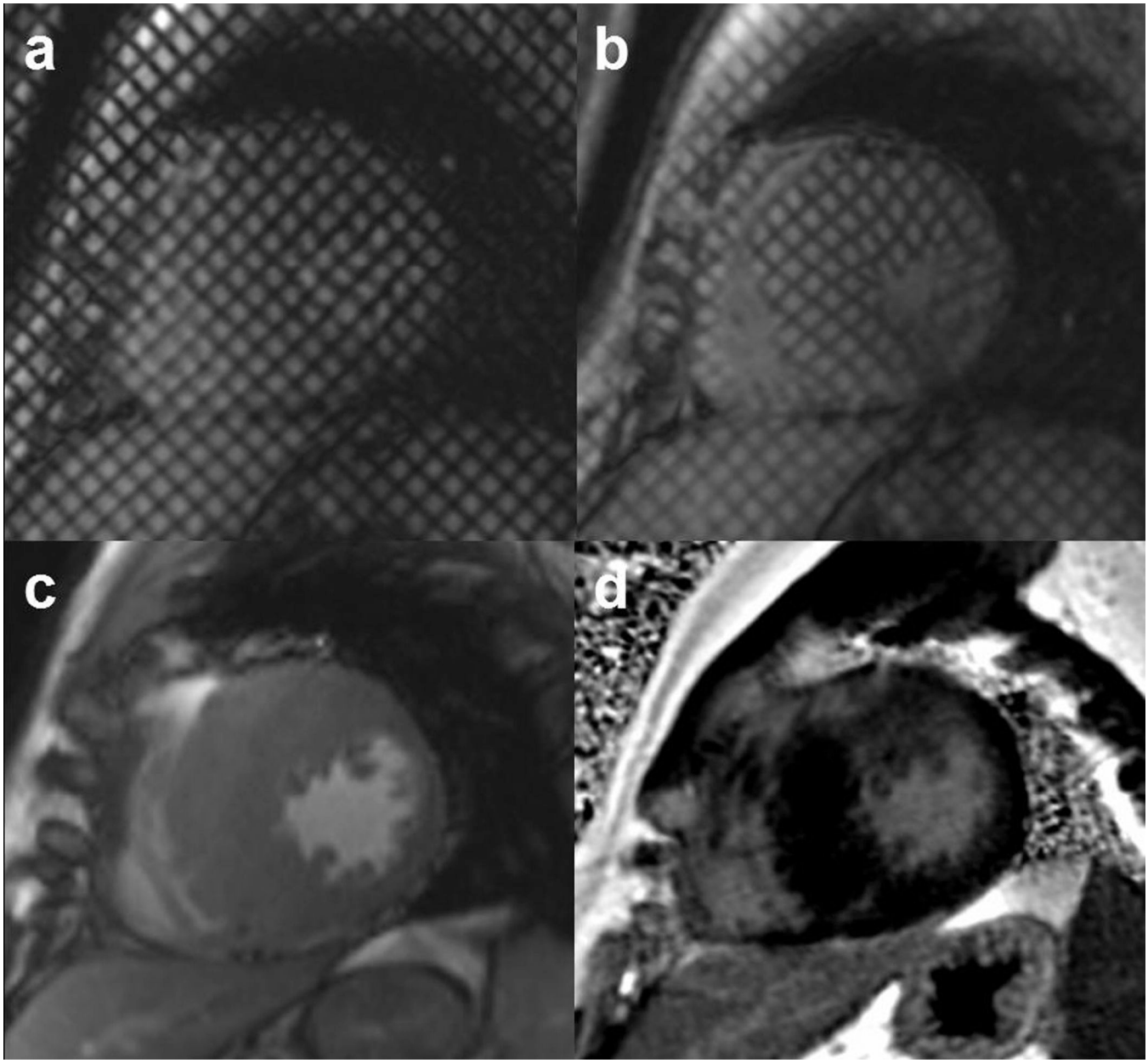

Figure 3.
CMR images from a 37 year old male with known HCM. Myocardial Tagging Images at (a) end diastole and (b) end systole demonstrate severe septal hypertrophy with minimal tag deformation in the anteroseptum. SSFP cine image (c) shows the asymmetric septal hypertrophy with a 3.6 cm wall thickness. Delayed enhanced image (d) shows a region of intramyocardial scarring in the anteroseptum near the RV insertion site, a pattern typically seen with HCM.

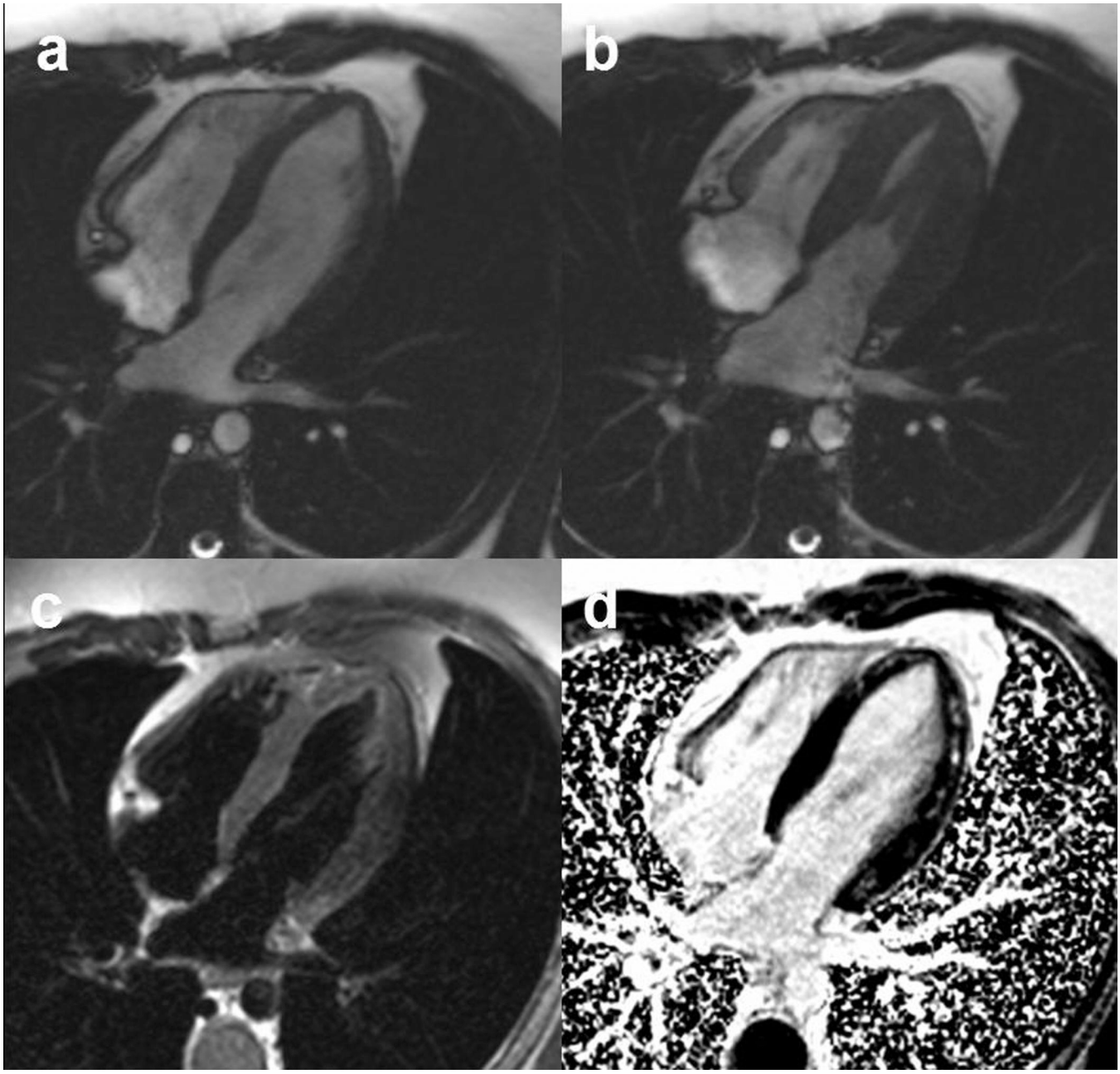

Figure 4.
CMR images from a 20 yo M admitted to an outside hospital with myocarditis who returns with recurrent chest pain. Cine SSFP images at (a) end diastole and (b) end systole demonstrate preserved systolic function. Edema imaging with (c) T2-weighted TSE does not show acute edema. Delayed enhancement images (d) demonstrate focal mid-wall scar in the lateral wall and apical-septal walls consistent with the clinical history of recent myocarditis.

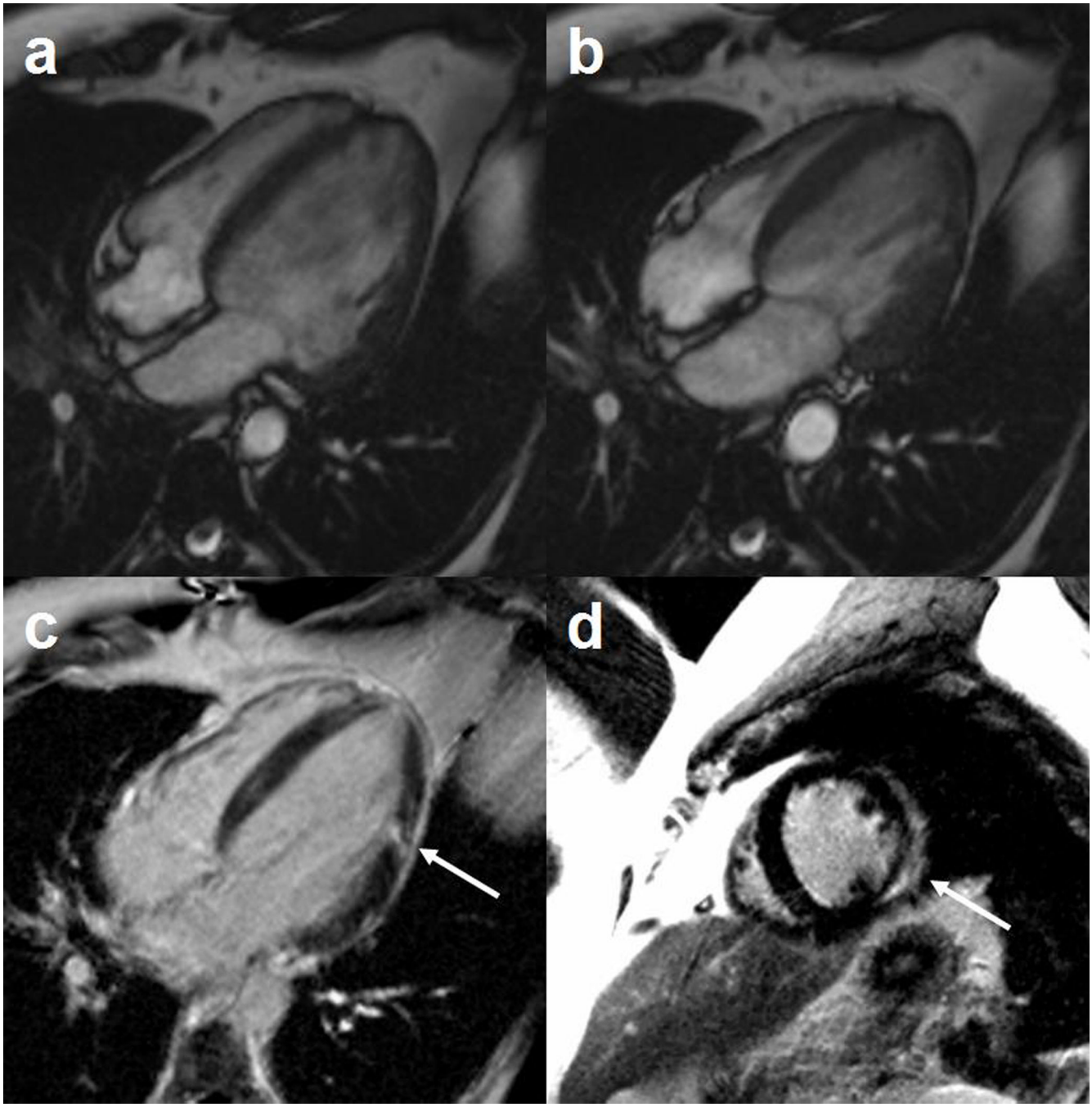

Figure 5.
CMR images from a 40 yo M with a history of biopsy proven pulmonary sarcoid with suspected cardiac involvement. Cine SSFP images at (a) end diastole and (b) end systole demonstrate reduced systolic function. Delayed enhancement images demonstrate focal mid-wall to epicardial scar in the lateral wall on (c) 4chamber and (d) short axis orientations.